Available online at www.sciencedirect.com
ScienceDirect

Trans. Nonferrous Met. Soc. China 24(2014) 893−899

Transactions of
Nonferrous Metals
Society of China

www.tnmsc.cn

Anodic behavior and microstructure of Al/Pb−Ag anode during zinc electrowinning

Yong-chun ZHANG[1], Bu-ming CHEN[1], Hai-tao YANG[1], Zhong-cheng GUO[1,2], Rui-dong XU[1]

1. Faculty of Metallurgy and Energy Engineering, Kunming University of Science and Technology,
Kunming 650093, China;
2. Kunming Hendera of Science and Technology Co. Ltd, Kunming 650106, China

Received 6 March 2013; accepted 5 November 2013

Abstract: Anodic behaviors and oxygen evolution kinetics of Pb−0.8%Ag and Al/Pb−0.8%Ag anodes during the initial 24 h zinc electrowinning were investigated with cyclic voltammetry (CV) curves and electrochemical impedance spectroscopy (EIS). The results reveal that the anodic behaviors and reaction kinetics of the two anodes vary a lot during the anodic polarization which indicate the formation and stabilization of anodic layer. Compared with conventional Pb−0.8%Ag anode, Al/Pb−0.8%Ag anode has longer time of anodic polarization. At the very beginning of anodic polarization, the two anodes all exhibit higher potential of oxygen evolution reaction (OER) since the reaction is controlled by the transformation step of intermediates. Then, its OER potential is largely diminished and OER rate is deduced from the formation and adsorption of the first intermediate ($S-OH_{ads}$). In the prolonged anodic polarization, the anodic potential of Al/Pb−0.8%Ag gradually decreases and the final value is more stable than that of conventional Pb−0.8%Ag anode. On the anodic layer after 24 h of anodic polarization, the OER potential is controlled by the formation and adsorption of intermediate. The microstructures of Al/Pb−0.8%Ag and Pb−0.8%Ag anodes after 24 h of anodic polarization were analyzed by scanning electron microscope (SEM).

Key words: zinc electrowinning; oxygen evolution kinetics; electrochemical impedance spectroscopy; oxygen evolution reaction potential

---

1 Introduction

The demand for energy-saving and higher standard of cathode zinc depends on the lower OER potential and corrosion rate of anodes used in zinc electrowinning. Lead based anodes have been used in the zinc electrowinning for more than a century due to their low cost and availability. However, the conventional lead based anodes operate at relatively high oxygen over-potential, which results in significant energy consumption, and suffer from corrosion which takes place at a slow rate during zinc electrowinning. Then researches [1−5] point that amount of silver (0.2%−1.0%) alloyed with lead decreases the oxygen overvoltage and increases the corrosion resistance of anodes used in zinc electrowinning. The polished surface of the Pb−0.69% Ag alloy anode has the lowest over-potential followed closely by that of Pb−0.6%Ag and Pb−0.58%Ag alloys anodes, showing that properties of conventional Pb−Ag anodes depend on their Ag content. The shape of anodes also can influence their properties. For instance, compared with conventional Pb−Ag anodes, porous Pb−Ag anodes save energy during initially zinc electrowinning [6,7], but their performances will be decreased when the non-conducting phases of MnO_2 and $PbSO_4$ are filled in their holes during zinc electrowinning. In addition, Ca, Bi, Co^{2+} and Mn^{2+} also can change the performances and anodic behaviors of conventional Pb−Ag anodes during zinc electrowinning [8−10].

Pb/Pb−Co_3O_4 [11−16] and Pb/Pb−MnO_2 [17−19] composite anodes have higher electro-catalytic activity and corrosion resistance for copper and zinc electrowinning. But the Co_3O_4 and MnO_2 particles are segregative during the preparation process of Pb−Co_3O_4 and Pb−MnO_2 composite coatings. So, the anodic processes are heterogeneous on the anodes during metal electrowinning, leading to shorter service time.

Foundation item: Project (51004056) supported by the National Natural Science Foundation of China

Corresponding author: Zhong-cheng GUO; Tel: +86-871-8352598; Fax: +86-871-8352599； E-mail: guozc012@163.com

DOI: 10.1016/S1003-6326(14)63140-X

WC, PANI, PbO_2 and CeO_2 particles which have been electrodeposited with Pb on aluminum-matrix are used as anodes in zinc electrowinning. Despite their higher corrosion resistance and electro-catalytic activity, Al/Pb−PANI−WC [20] and Al/α-PbO_2−CeO_2−TiO_2 anodes [21] are still the new anode materials in the laboratory. PANI and WC particles are non-uniform in composite anodes for segregation during the preparation of Al/Pb−PANI−WC and Al/α-PbO_2−CeO_2−TiO_2 composite anodes. PANI/WC anode prepared by pressing is easy to spit and peel off during the anodic polarization, leading to shorter service time. α-PbO_2−CeO_2−TiO_2 composite coating is also easy to peel off from the aluminum matrix due to the characteristics of α-PbO_2.

Aluminum has a lower cost, density and electrical resistivity than lead, which can possibly reduce the bath voltage and mass of aluminum-based anodes for zinc electrowinning.

In this work, Al/Pb−0.8%Ag anode was prepared by electrodeposition from a synthetic lead methanesulfonate electrolyte. These researches present the results of a study which aims to extend the new work and utilize some of the benefits of Al-matrix and Pb−0.8%Ag composite coating. Therefore, the goal is to develop a new method for preparation of Pb−0.8%Ag composite anode which can offer improved performance in zinc electrowinning.

2 Experimental

2.1 Process method

The alloy materials were obtained by electrodeposition on 30 mm×40 mm aluminum plates from a synthetic lead methanesulfonate electrolyte consisting of 0.5−2 g/L organic additives, 100−200 g/L $Pb(CH_3SO_3)_2$ and 0.5−1 g/L $AgCH_3SO_3$. The electro deposition was carried out at pH values in the range of 1.5−2 at a cathode current density J_c=1 A/dm^2 with mechanical bubbling for 24 h at 40 °C.

The aluminum-matrix was pretreated by buffing (mechanical buffing with fiber grinding wheel), degreasing (soak in fatty alcohol-polyoxyethylene ether degreaser at 40 °C for 4−12 h), caustic wash (soak in 12 g/L NaOH solution at 20−40 °C for 120−180 s), acid pickling (38 g/LH_2SO_4 at 20−40 °C for 10−30 s), zinc immersion (soak in 12 g/L NaOH, 15 g/L ZnO, 10 g/L $KNaC_4H_4O_6\cdot 4H_2O$, 2 g/L $FeCl_3\cdot 6H_2O$ solution at 20−40 °C for 60 s), acid pickling (3−10 s), zinc immersion (at 20−40 °C for 50 s) and nickel electroplating for 1 min.

2.2 Measurement and analysis

The electrochemical workstation (CHI760C) with three-electrode systems was used for measuring cyclic voltammetry curves and EIS characterization for Al/Pb−0.8%Ag and conventional Pb−0.8%Ag anodes in the synthetic zinc electrowinning electrolyte consisting of Zn^{2+}(50 g/L), H_2SO_4 (150 g/L) and Mn^{2+} (5 g/L). The counter electrode was platinum plate and the reference electrode was Hg/Hg_2SO_4 electrode (SSE) with a potential φ_{SSE}=+0.64 V. The two anodes were used as the working electrode. In addition, SEM and XRD were used for determining surface microstructure and phase of the two anodes after 24 h anodic polarization.

The anodic polarization was performed at 500 A/cm^2 in a glass at a constant temperature of 35 °C. The CV scanning rate was 30 mV/s and the range of CV scanning was from −1.2 to 2.0 V. The frequency range of EIS measuring was 0.01−10 kHz and the applied anodic potential for EIS measuring was 1.85 V.

3 Results and discussion

3.1 Cyclic voltammetry curves

As shown in Figs. 1 and 2, cyclic voltammetry curves of conventional Pb−0.8%Ag (Fig. 1) and Al/Pb−0.8%Ag (Fig. 2) anodes after 0, 12 and 24 h anodic polarization are nonreversible, so Eq. (1) obtained by BARD and FAULKNER [22] can be used in this case. Classic Butler−Volmer kinetics model which is necessary before equations can be derived for most electrochemical approaches apply in this part, then a plot of ln$k_f(\varphi)$ versus φ should be line with a slope $(-\alpha F/RT)$. Based on researches of Refs. [23,24] and Frank−Condon principle, Eq. (2) can be obtained and α depends on potential in a particular way.

$$\ln k_f(\varphi) = \ln D_o^{1/2} - \ln\frac{[I_1 - I(t)]}{i(t)} \tag{1}$$

$$\alpha = \frac{1}{2} + \frac{F(\varphi' - \varphi^{\Theta})}{2\lambda} \tag{2}$$

where $k_f(\varphi)$ is the potential-dependent rate constant as a function of potential φ; φ' is an electrode versus a

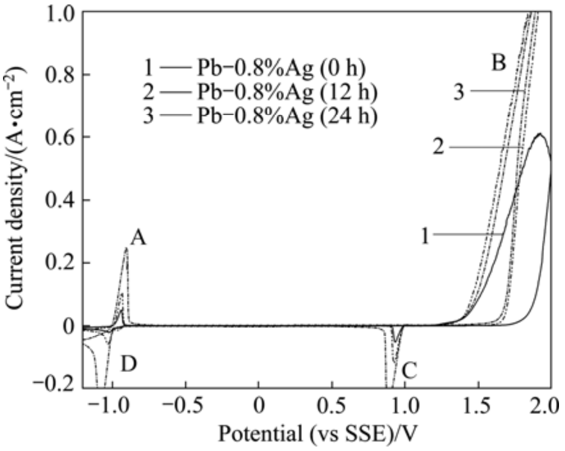

Fig. 1 Cyclic voltammetry curves of conventional Pb−0.8%Ag anode after 0, 12 and 24 h of anodic polarization

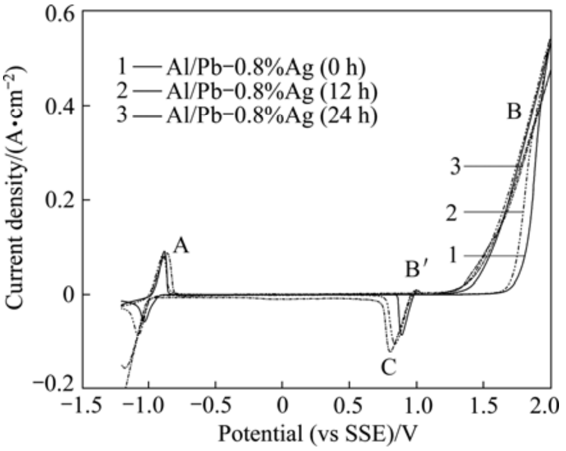

Fig. 2 Cyclic voltammetry curves of Al/Pb−0.8%Ag anode after 0, 12 and 24 h of anodic polarization

reference at different scanning speed v; k_f is the heterogeneous rate constant for reduction; D_o is the diffusion coefficient of O; $I(t)$ is the current semi-integral; I_l is the limit value of $I(t)$; $i(t)$ is the experimental current; F is the faraday constant; E' is the electron energy, E^{Θ} is the standard potential of an electrode or couple; α is the transfer coefficient.

Reorganization energy for electron transfer λ can be obtained as follows:

$$\lambda = \lambda_i + \lambda_0 \tag{3}$$

where λ_i is the contribution from reorganization of species O; and λ_0 is the contribution from reorganization of the solvent.

Considering electrode reaction and ignoring self-exchange reaction and λ_i, equation can be obtained as follows [22]:

$$\lambda = 2\Delta G_f^{\Theta} \tag{4}$$

where ΔG_f^{Θ} is the standard Gibbs free energy of forward action.

In this case, $i(t)$ is probably related to the pretreatment of the aluminum matrix and the type of additives in the electrolyte used for the preparation of composite coatings, and D_o is probably related to the microstructure of anodic layer of the two anodes during anodic polarization. The CV scanning rates for Pb−0.8%Ag and Al/Pb−0.8%Ag anodes are all 30 mV/s. The higher electrocatalytic activity can promote the anode reaction, and the OER potential and ΔG_f^{Θ} of anode reaction decrease. So, α increases and $-\alpha F/(RT)$ decreases.

As shown in Fig. 1, the curves of Pb−0.8%Ag anode after 0, 12 and 24 h of anodic polarization show two anodic peaks and two cathodic peaks [25,26]. The first peak A is produced by the reaction as follows:

$$\mathrm{Pb} + \mathrm{SO_4^{2-}} - 2\mathrm{e} \rightarrow \mathrm{PbSO_4} \tag{5}$$

A well shape passive region ensues, followed by PbO_2 formation and oxygen evolution peak B. In this peak only β-PbO_2 is formed, as shown by absence of a divided reaction peak C [27]. The division of the peak can be attributed to the presence of two phases, α-PbO_2 and β-PbO_2. After 12 h of anodic polarization (curve 2), the lead sulphate area of peak A is the shifting of this peak to positive potential values, but that of peak B is the shifting to negative potential values. So, the area from lead sulphate to β-PbO_2 is decreased. After 24 h of anodic polarization (curve 3), the area from lead sulphate to β-PbO_2 is narrower than curve 2. At the reverse scanning, the potential values of peaks C and D are the shifting of this peak to more positive with an increase of anodic polarization time, the reduction peaks C and D are also increased by a higher peak and increase the width of the passive zone, leading to the longer time of anodic polarization.

As shown in Fig. 2, anodic behaviors of Al/Pb−0.8%Ag anode are similar to Pb−0.8%Ag anode after 0, 12 and 24 h of anodic polarization. With the increase of anodic polarization time, the peak A is the shifting of this peak to positive potential values and peak B is the shifting to negative potential values, leading to narrower area from lead sulphate to β-PbO_2. At the reverse scanning, the potential values of peaks C and D are the shifting of this peak to more positive, the reduction peaks C and D are also increased by a higher peak and increase the width of the passive zone, leading to the longer time of anodic polarization. However, the peak B area of Al/Pb−0.8%Ag anode is narrower than Pb−0.8%Ag anode, which is due to its lower oxygen evolution reaction potential.

As shown in Fig. 3, Al/Pb−0.8%Ag anode has longer time of anodic polarization than Pb−0.8%Ag anode after 24 h of anodic polarization in lower potential zone, which is probably due to the different surface resistances. The surface resistance is probably related to the β-PbO_2 phase and microstructure of the two anodes.

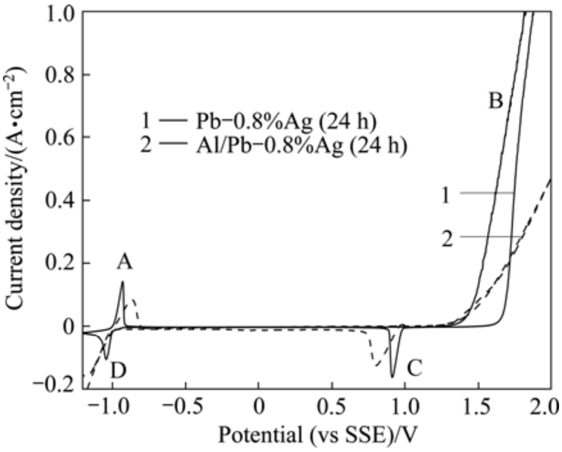

Fig. 3 Cyclic voltammetry curves of Pb−0.8Ag and Al/Pb−0.8%Ag anodes after 24 h of anodic polarization

3.2 EIS characterization

Figure 4 shows the typical potential−time curves of Pb−0.8%Ag (curve 1) and Al/Pb−0.8%Ag (curve 2) anodes during the beginning 24 h of anodic polarization. Al/Pb−0.8%Ag anode exhibits excellent electro-catalytic activity towards oxygen evolution reaction during the beginning 24 h of anodic polarization. The activity diminishes largely due to the change of the surface state for new microstructure and phase. In the prolonged anodic polarization, the anodic potential gradually decreases and the potential is lower than Pb−0.8%Ag anode after 24 h of anodic polarization. The whole anodic polarization process can be expressed by the following formation of $PbSO_4$ and PbO_2 phases. The two anodes have different anodic behaviors during 24 h of anodic polarization which can be studied with EIS. As shown in Fig. 5, the new phase β-PbO_2 is found on the surface of the two anodes after 24 h of anodic polarization. So, the conclusion can be deduced that β-PbO_2 phase has been produced during the initial 24 h of anodic polarization.

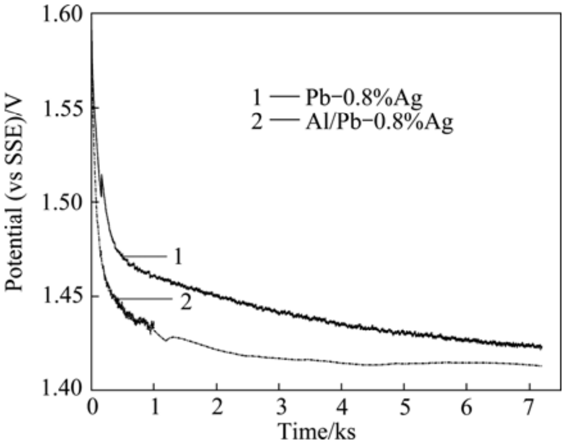

Fig. 4 Time−potential curves of Pb−0.8%Ag and Al/Pb−0.8%Ag anodes during 24 h anodic polarization

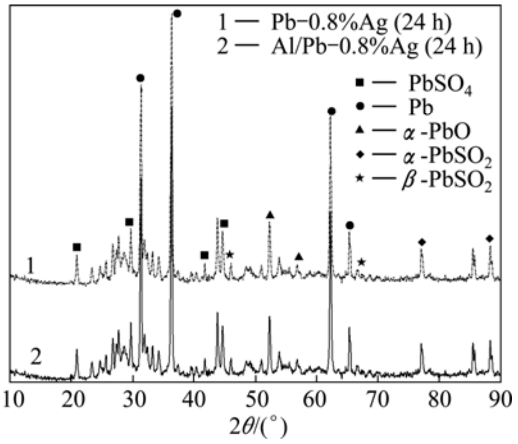

Fig. 5 XRD patterns of Pb−0.8%Ag and Al/Pb−0.8%Ag anodes after 24 h of anodic polarization

The oxygen evolution reaction steps are generally proposed as the mechanism of OER on active metal oxides electrode [28,29]. The oxygen evolution reaction by decomposition of water in acid medium can be described as follows:

$$2H_2O-4e\rightarrow 4H^++O_2 \tag{6}$$

$$S+H_2O\rightarrow S-OH_{ads}+H^++e \tag{7}$$

$$S-OH_{ads}\rightarrow S-O_{ads}+H^++e \tag{8}$$

$$2S-OH_{ads}\rightarrow S-O_{ads}+S+H_2O \tag{9}$$

$$S-O_{ads}\rightarrow S+O_2/2 \tag{10}$$

where S stands for active site on oxide surface, $S-OH_{ads}$ and $S-O_{ads}$ are adsorption intermediates. Reaction (8) is normally considered to be obeyed by compact morphology and reaction (9) is obeyed by cracked morphology. In addition, reaction (10) generates O_2. According to the mechanism discussed above, the oxygen evolution reaction is kinetically controlled by Eq. (1) through reactions (7)−(10) during 24 h anodic polarization. Based on the faradic impedance Z_f of such irreversible electrode reactions with one state variable besides electrode potential can be written as follows:

$$Z_f=R_t+\frac{R_a}{1+j\omega R_aC_a} \tag{11}$$

where R_t is the charge transfer resistance of the electrode reaction and always has a positive value; R_a and C_a are the equivalent resistance and pseudo-capacitance associated with adsorption of intermediate ($S-OH_{ads}$), respectively. As shown in Fig. 6, C_{dl} is the double-layer capacitance and R_s is the uncompensated solution resistance. By theoretical calculation, R_fC_f represents the capacitive response of oxide layer, R_f and C_f are the resistance and capacitance of the oxide layer, respectively. In the simulation, constant phase elements (CPEs) are used instead of capacitors, C_{dl} and C_a, to fit the experimental data. The CPE can obtain a good approach to the surface roughness, physical non-uniformity or the non-uniform distribution of surface reaction site. The impedance CPE can be written as

$$Z_{CPE}=\frac{1}{Q(j\omega)^n} \tag{12}$$

where Q is the capacity parameter and n is accounting for the deviation from the ideal behaviors. Moreover, the double layer capacitance C_{dl} is coupled with the uncompensated solution resistance R_s and the charge transfer resistance R_t according to the equation as follows [30]:

$$Q_{dl}=(C_{dl})^n\left[(R_s)^{-1}+(R_t)^{-1}\right]^{(1-n)} \tag{13}$$

The simulated EIS patterns and parameters of Pb−0.8%Ag and Al/Pb−0.8%Ag anodes are shown in Figs. 6 and 7. In the simulation of those spectra with one capacity arc, it shows that the simulated and experimental data can reach a good agreement by the proper circuit in Fig. 8. Such phenomenon may be explicable below. It has been wildly proposed that the formation of anodic layer on lead-based anode is mainly according to the following two processes: 1) Pb$\rightarrow$PbSO$_4$$\rightarrow$$\beta$-PbO$_2$; 2) Pb$\rightarrow$PbSO$_4$$\rightarrow$$\alpha$-PbO$_2$$\rightarrow$$\beta$-PbO$_2$. Therefore, during the formation process of anodic layer, considerable layer resistance exists probably due to non-conducting PbSO$_4$ and α-PbO$_2$. As listed in Table 1, the charge transfer resistance R_t only takes little part of the whole resistance in this case, while the film resistance R_f and adsorption resistance R_a dominantly determine the final resistance values. In general, the sum of R_f and R_a values of the two anodes largely decrease during anodic polarization, indicating that the adsorption of intermediate becomes easier with the PbO$_2$ layer. The film resistance of Pb−0.8%Ag anode is larger than Al/Pb−0.8%Ag anode. Moreover, the change of Pb−0.8%Ag anode adsorption resistance is different from that of Al/Pb−0.8%Ag anode adsorption resistance during the 24 h of anodic polarization. It also has the lowest adsorption resistance on its fruit surface which is due to the different microstructures.

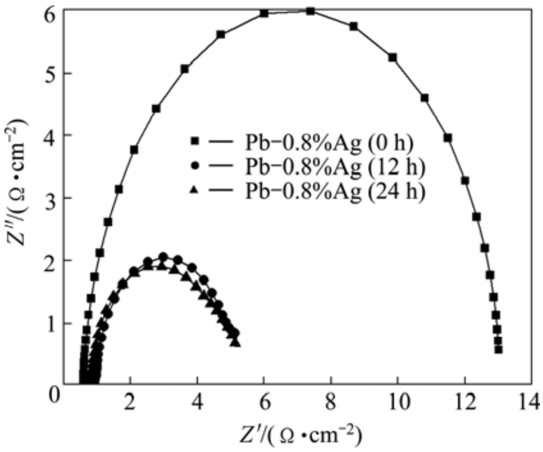

Fig. 6 EIS of Pb−0.8%Ag anode after fitting

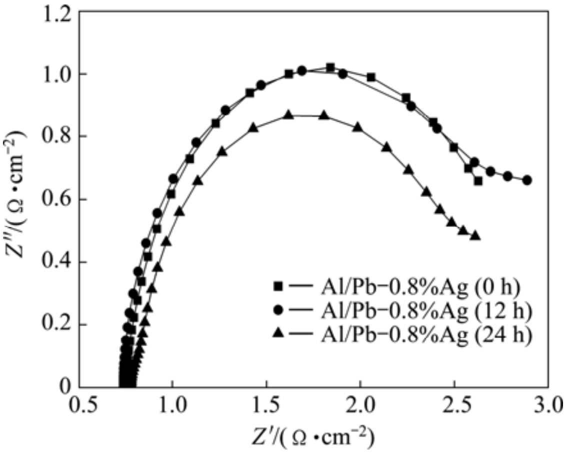

Fig. 7 EIS of Al/Pb−0.8%Ag anode after fitting

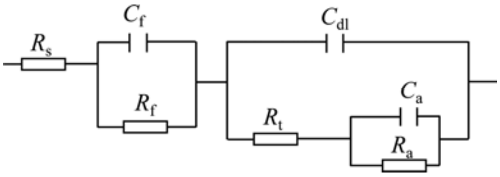

Fig. 8 Electrical equivalent circuit used to simulate impedance

In addition, the double layer capacitance C_{dl} is calculated by Eq. (13). As listed in Table 1, the generally increasing C_{dl} values of the two anodes reveal that the anodic surface becomes more prone to the adsorption of anions by prolonging the time of anodic polarization. The behavior of adsorption pseudo-capacitance during the anodic polarization is evaluated by the Q_{dl} values obtained in the CNLS fit. Since the pseudo-capacitance represents the coverage of intermediate on the anodic surface, its generally increasing trend during the anodic polarization indicates that the intermediate S−OH$_{ads}$ can be more easily adsorbed on the stable PbO$_2$ layer as well. Besides，between the two anodes, Al/Pb−0.8%Ag anode presents larger Q_{dl} values in latter anodic polarization which is probably due to the thick, micro-porous(as shown in Fig. 9) and β-PbO$_2$-rich anodic layer, showing higher corrosion resistance and electro-catalytic activity.

Table 1 Equivalent circuit parameters for Pb−0.8%Ag and Al/Pb−0.8%Ag anodes

Anode	R_s/ (Ω·cm^{-2})	C_f/ (10^{2}F·cm^{-2})	R_f/ (Ω·cm^{-2})	C_{dl}/ (F·cm^{-2})	R_t/ (Ω·cm^{-2})	Q_{dl}/ (Ss^n·cm^{-2})	n	R_a/ (Ω·cm^{-2})
Pb−0.8%Ag (0 h)	0.61	1.17	14.77	58	0.48	53.4	0.97	0.49
Pb−0.8%Ag (12 h)	0.921	3.73	3.96	31	0.079	28.6	0.90	1.23
Pb−0.8%Ag (24 h)	0.85	3.58	3.46	290	0.044	249.7	0.94	1.00
Al/Pb−0.8%Ag (0 h)	0.76	4.42	1.92	190	0.054	166.0	0.94	9.68
Al/Pb−0.8%Ag (12 h)	0.74	6.48	1.84	540	0.091	414.5	0.93	0.89
Al/Pb−0.8%Ag (24 h)	0.88	9.56	1.64	150	0.062	294	0.87	0.63

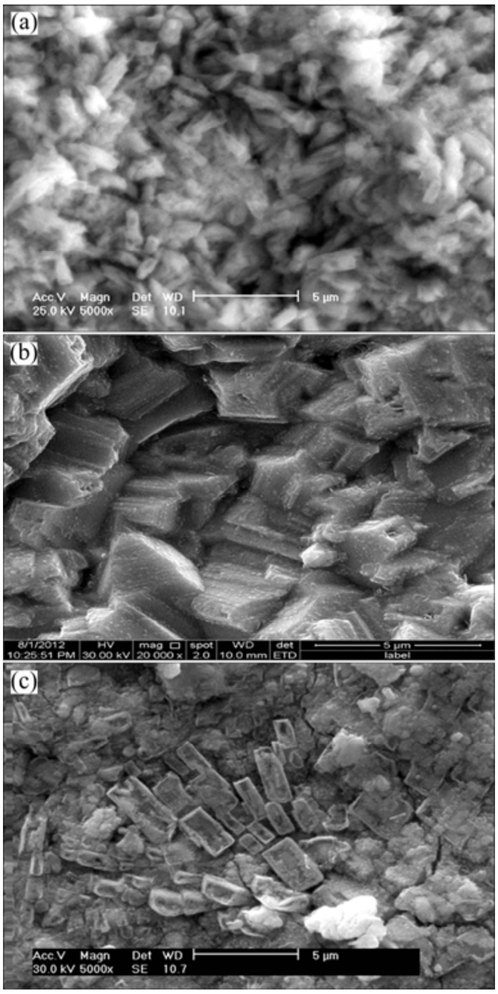

Fig. 9 SEM images of Pb−0.8%Ag anode after 24 h of anodic polarization (a) and Al/Pb−0.8%Ag anode before (b) and after (c) 24 h of anodic polarization

As shown in Fig. 9, the SEM images of Pb−0.8%Ag anode after 24 h of anodic polarization and Al/Pb−0.8%Ag anode before and after 24 h of anodic polarization are shown clearly. The microstructure of Al/Pb−0.8%Ag anode after 24 h of anodic polarization (Fig. 9(c)) is characterized by rectangular crystallites of $PbSO_4$, possessing an order orientation and concentrating. The microstructure of Pb−0.8%Ag anode after 24 h of anodic polarization (Fig. 9(a)) is characterized by irregular crystallites of $PbSO_4$, possessing a uniform tetragonal symmetry and chaotic orientation [24] which is probably conducive to the diffusion of O_2. The results above are probably due to the microstructure of Al/Pb−0.8%Ag anode (see Fig. 9(b)) and its aluminum-matrix.

4 Conclusions

1) Compared with conventional Pb−0.8%Ag anode, Al/Pb−0.8%Ag anode has longer time of anodic polarization, and the microstructure on anodic layer is characterized by rectangular crystallites of $PbSO_4$, processing an order orientation after 24 h anodic polarization which is probably due to the preparation method for Al/Pb−0.8%Ag anode and its aluminum-matrix.

2) At the beginning of anodic polarization, Al/Pb−0.8%Ag anode firstly presents fairly high OER potential controlled by the transformation of intermediate due to the existence of non-conducting phases of MnO_2 and α-PbO_2. After 24 h anodic polarization, the film impedance nearly disappears and the reaction resistance is dominantly composed by the adsorption resistance. The adsorption resistance and pseudo-capacitance of the Al/Pb−0.8%Ag anode are much smaller and larger than those of Pb−0.8%Ag anode, respectively. Such phenomenon can be well interpreted by XRD analysis on these stable anodic layers, which show that Al/Pb−0.8%Ag anode presents obviously more conducting and active β-PbO_2 phase on the anodic layer.

3) Compared with conventional Pb−0.8%Ag anode, Al/Pb−0.8%Ag anode has lower surface resistance and larger Q_{dl} due to the more β-PbO_2 phase, showing higher corrosion resistance.

References

[1] ZHANG W, HOULACHI G. Electrochemical studies of the performance of different Pb−Ag anodes during and after zinc electrowinning [J]. Hydrometallurgy, 2010, 104(2): 129−135.

[2] CACHAT C, REROLLE C. Kinetics of oxygen evolution on Pb and Pb−Ag anodes during zinc electrowinning [J]. Electrochimica Acta, 1996, 41(7): 1063−1069.

[3] RASHKOV S T, STEFANOV Y, NONCHEVA Z. Investigation of the processes of obtaining plastic treatment and electrochemical behaviour of lead alloys in their capacity as anodes during the electroextraction of zinc II. Electrochemical formation of phase layers on binary Pb−Ag and Pb−Ca, and ternary Pb−Ag−Ca alloys in a sulphuric-acid electrolyte for zinc electroextraction [J]. Hydrometallurgy, 1996, 40(3): 319−334.

[4] HYVARINEN O, TIKKANEN M N. On the anodic behaviour of lead-silver alloys in sulphuric acid solution [J]. Acta Polytech Scand, 1969, 89: 5−20.

[5] ZHANG W, YIFENG C, EDWARD G, GEORGES H. Effects of Ag content in lead anodes on oxygen evolution during zinc electrowinning [C]//New York: 2012 International Conference on Power and Energy Systems (ICPES), 2012: 311−317.

[6] LAI Yan-qing, JIANG Liang-xing, LI Jie, ZHONG Shui-ping, LÜ Xiao-jun, PENG Hong-jian, LIU Ye-xiang. A novel porous Pb−Ag anode for energy-saving in zinc electro-winning: Part II: Laboratory preparation and properties [J]. Hydrometallurgy, 2010, 102(1): 81−86.

[7] LAI Yan-qing, JIANG Liang-xing, LI Jie, ZHONG Shui-ping, LÜ Xiao-jun, PENG Hong-jian, LIU Ye-xiang. A novel porous Pb–Ag anode for energy-saving in zinc electro-winning: Part I: Laboratory preparation and properties [J]. Hydrometallurgy, 2010, 102(1): 73−80.

[8] PRENGAMAN R D, SIEGMUND A. New wrought Pb−Ag−Ca anodes for zinc electrowinning to produce a protective oxide coating

rapidly [C]//New York: U.S. Lead In C. 2000 Symposium, 2000, 589−596.

[9] ZHONG S P, LAI Y Q, JIANG L X, TIAN Z L, LI J, LIU Y X. Electrchemical behavior of Pb−Ag−Bi alloys as anode in zinc electrowinning [J]. Journal of Chinese Process Engeering, 2008, 8(1): 289−293. (in Chinese)

[10] CACHET C, LE PAPE-REROLLE C, WIART R. Influence of Co^{2+} and Mn^{2+} ions on the kinetics of lead anodes for zinc electrowinning [J]. Journal of Applied Electrochemistry, 1999, 29(7): 813−820.

[11] HRUSSANOVA A, MIRKOVA L, DOBREV T S, VASILEV S. Influence of temperature and current density on oxygen overpotential and corrosion rate of Pb−Co_3O_4, Pb−Ca−Sn, and Pb−Sb anodes for copper electrowinning: Part I [J]. Hydrometallurgy, 2004, 72(3): 205−213.

[12] HRUSSANOVA A, MIRKOVA L, DOBREV T S. Influence of temperature and current density on oxygen overpotential and corrosion rate of Pb−Co_3O_4, Pb−Ca−Sn, and Pb−Sb anodes for copper electrowinning: Part Π [J]. Hydrometallurgy, 2004, 72(3): 215−224.

[13] HRUSSANOVA A, MIRKOVA L, DOBREV T S. Electrochemical properties of Pb−Sb, Pb−Ca−Sn and Pb−Co_3O_4 anodes in copper electrowinning [J]. Journal of Applied Electrochemistry, 2002, 32(5): 505−512.

[14] MARYAM J B, ALEKSANDAR N N. Electrodeposition of lead-cobalt composite coatings electrocatalytic for oxygen evolution and the properties of composite coated anodes for copper electrowinning [J]. Hydrometallurgy, 2012, 129: 59−66.

[15] HRUSSANOVA A, MIRKOVA L, DOBREV T. Anodic behavior of the Pb−Co_3O_4 composite coating in copper electrowinning [J]. Hydrometallurgy, 2001, 60(3): 199−213.

[16] KONG Ying, XU Rui-dong, HUANG Li-ping, GUAN Yong-yong. Electrochemical properties of Pb−0.3Ag/Pb−Co_3O_4 composite inert anodes [J]. The Chinese Journal of Material Research, 2012, 26(5): 495−502. (in Chinese)

[17] SONKE S, MARTINA T, KYOSTI K, OLOF F, MICHAEL H B. New oxygen evolution anodes for metal electrowinning: MnO_2 composite electrodes [J]. Journal of Applied Electrochemistry, 2009, 39(10): 1835−1848.

[18] SONKE S, SASCHA E P, KYOSTI K, OLOF F, GUNTHER W. New oxygen evolution anodes for metal electrowinning: Investigantion of local physicochemical processes on composite electrodes with conductive atomic force microscopy and scanning electrochemical microscopy [J]. Journal of Applied Electrochemistry, 2010, 40(3): 581−592.

[19] LAI Yan-qing, JIANG Liang-xing, LI Jie, ZHONG Shui-ping, LÜ Xiao-jun, PENG Hong-jian, LIU Ye-xiang. Electrochemical behavior of co-deposited Pb/Pb−MnO_2 composite anode in sulfuric solution−Tafel and EIS investigations [J]. Journal of Electroanalytical Chemistry, 2012, 671: 16−23.

[20] XU Rui-dong, HUANG Li-ping, ZHOU Jian-feng, ZHAN Peng, GUAN Yong-yong, KONG Ying. Effects of tungsten cabide on electrochemical properties and microstructural feature of Al/Pb−PANI-WC composite inert anodes used in zinc electrowinning [J]. Hydrometallurgy, 2012, 125: 8−15.

[21] CHEN Bu-ming, GUO Zhong-cheng, XU Rui-dong. Electrosynthesis and physicochemical properties of α-PbO_2–CeO_2–TiO_2 composite electrodes [J]. Transactions of Nonferrous Metals Society of China, 2013, 23(4): 1191−1198.

[22] BARD A J, FAULKNER L R. Electrochemical methods: Fundamentals and application [M]. New York: John Wiley & Sons, 2000: 226−247.

[23] MARCUS R A, SIDDARTH P, KOCHANSKI E. Photoprocesses in transition metal complexes, biosystems and other molecules experiment and theory [M]. New York: Kluwer Amsterdam, 1992: 273−275.

[24] da SILVA L A, ALVES V A, TRASATTI S. Surface and electrocatalytic properties of ternary oxides Ir0.3Ti(0.7−x)Pt$x$$O_2$ oxygen evolution from acidic solution [J]. Journal of Electroanalytical Chemistry, 1997, 427(1−2): 97−104.

[25] YAMAMOTO Y, FUMINO K, UEDA T. A potentiodynamic study of the lead electrode in sulphuricacid solution [J]. Eletrochimica Acta, 1992, 37(2): 199−203.

[26] LAITINEN T, MONAHOV B, SALMI K. Ring-disk electrode studies of soluble intermediates formed during the polarization of Pb in H_2SO_4 [J]. Eletrochimica Acta, 1991, 36(5): 953−963.

[27] PETROVA M, STEFANOV Y, NONCHEVA Z. Electrochemical behaviour of lead alloys as anodes in zinc electrowinning [J]. British Corrosion Journal, 1991, 34(3): 198−200.

[28] da SILVA L M, BOODTS J F C, de FARIA L A. Oxygen evolution at $RuO_2(x)+Co_3O_4(1-x)$ electrode from acid solution [J]. Eletrochimica Acta, 2001, 46(9): 1369−1375.

[29] AROMAA J, FOESEN O. Evaluation of the electrochemical activity of a Ti−RuO_2−TiO_2 permanent anode [J]. Eletrochimica Acta, 2006, 51(27): 6104−6110.

[30] BRUG G J, VANDEN EEDEN A L G, SLUYTERS-REHBACH M, SLUYTERS J H. The analysis of electrode impedances complicated by the presence of a constant phase element [J]. Journal of Electroanalytical Chemistry, 1984, 176(1): 275−295.

Al/Pb−Ag 阳极在锌电积过程中的阳极行为和微观结构

张永春 [1]，陈步明 [1]，杨海涛 [1]，郭忠诚 [1,2]，徐瑞东 [1]

1. 昆明理工大学 冶金与能源工程学院，昆明 650093；2. 昆明理工恒达科技有限公司，昆明 650106

摘 要：采用循环伏安曲线(CV)和电化学交流阻抗谱(EIS)研究 Pb−0.8%Ag 和 Al/Pb−0.8%Ag 阳极在最初 24 h 锌电积过程中的阳极行为和析氧动力学。结果表明：2 种阳极材料在阳极极化过程中的阳极行为和动力学的多种变化表明阳极表面膜的形成和稳定。与传统的 Pb−0.8%Ag 阳极相比，Al/Pb−0.8%Ag 阳极具有较长的极化时间。 在最初的电积过程中，阳极表面中间产物的转变使 2 种阳极都表现出较高的析氧电位。随着析氧电位降低，析氧反应速率可以由阳极表面最初的生成物和中间产物 S−OH_{ads} 推断。随着电积的持续进行，Al/Pb−0.8%Ag 阳极的析氧电位逐渐降低，Al/Pb−0.8%Ag 阳极比 Pb−0.8%Ag 阳极先达到稳定状态。电积 24 h 后，阳极电位由阳极表面的生成物和中间产物控制。采用扫描电子显微镜观察 Al/Pb−0.8%Ag 和 Pb−0.8%Ag 阳极锌电积 24 h 后的微观形貌。

关键词：锌电积；析氧动力学；电化学交流阻抗；析氧电位

(Edited by Chao WANG)